


A novel 3D anatomic mapping approach using multipoint high-density voltage gradient mapping to quickly localize and terminate typical atrial flutter

William C. Choe¹  · Sri Sundaram¹ · J. Ryan Jordan¹ · Nate Mullins² · Charles Boorman² · Austin Davies² · Alex C. Tiftickjian³ · Sunil Nath⁴

Received: 13 April 2017 / Accepted: 14 July 2017 / Published online: 22 July 2017
© Springer Science+Business Media, LLC 2017

Abstract

Purpose The purposes of the study were to evaluate and characterize the cavotricuspid isthmus using multipoint high density voltage gradient mapping (HD-VGM) to see if this would improve on current ablation techniques compared to standard cavotricuspid isthmus ablation techniques.

Methods Group 1, 25 patients who underwent ablation using standard methods of 3D mapping and ablation, was compared to group 2, 33 patients undergoing ablation using HD-VGM and ablation. Using this method, we are able to identify the maximum voltage areas within isthmus and target it for ablation. Total procedure times, ablation times and number of lesions, distance ablated, and fluoroscopy times were compared.

Results Fifty-eight patients were included in this study. Compared to group 1, in group 2, HD-VGM decreased the total ablation time 18.2 ± 9.2 vs 8.3 ± 4.0 min ($p < 0.0001$), total ablation lesions 22.7 ± 18.8 vs 5.5 ± 4.2 ($p < 0.0001$), and the length of the ablation lesions was significantly shorter $47.0 \text{ mm} \pm 13 \text{ mm}$ vs $32.6 \text{ mm} \pm 10.0 \text{ mm}$ ($p < 0.0001$). While the average length of the CTI was similar, $47.0 \text{ mm} \pm 13 \text{ mm}$ vs $46.1 \text{ mm} \pm 10.0 \text{ mm}$ ($p 0.87$), in group 2, only 71% of the isthmus was ablated.

Conclusion Multipoint high density voltage gradient mapping can help identify maximum voltage areas within the isthmus and when ablated can create bidirectional block with decreased ablation times and length of the lesion.

Keywords Typical atrial flutter · Radiofrequency ablation · 3D anatomic mapping · High density mapping · Voltage gradient mapping · Catheter ablation

Abbreviations

AF	Atrial fibrillation
HD-VGM	High density activation sequence mapping with voltage gradient mapping
AFL	Typical atrial flutter
LA	Left atrium
RA	Right atrium
CS	Coronary sinus
LAT	Local activation timing
RAI	Roving activation interval
Low V ID	Low voltage identification
RF	Radiofrequency

1 Introduction

Typical atrial flutter (AFL) has been recognized as a distinct clinical arrhythmia for over 100 years [1–3]. Typical AFL is a reentrant circuit rotating in a counterclockwise (CCL) fashion around the right atrium (RA) funneling through a narrow channel between the inferior vena cava (IVC) and tricuspid valve (TV) with passive activation of the left atrium. The cavotricuspid isthmus (CTI) has been identified as the critical zone of slow conduction for the maintenance of typical AFL [4, 5]. Fluoroscopic imaging

✉ William C. Choe
williamc@southdenver.com

¹ South Denver Cardiology Associates, 1000 South Park Drive, Littleton, CO 80120, USA

² St Jude Medical, St Paul, MN, USA

³ Porter Adventist Hospital, Denver, CO, USA

⁴ Colorado Springs Cardiologists, Colorado Springs, CO, USA

is traditionally combined with 3D mapping to position the ablation catheter at 6 o'clock on the TV in the LAO 30° view. A continuous radiofrequency ablation line performed transecting the TV to the IVC in this area will terminate the tachycardia. [6, 7] Achieving bidirectional block is considered the standard for success with low recurrence rates. [7–9] By using high density (HD) mapping of the CTI with a 3D mapping system, multiple points can be acquired simultaneously at each catheter position allowing for a more accurate activation and voltage map of the area of interest in a short period of time. This study reports a novel method utilizing high density activation sequence mapping combined with voltage gradient mapping (HD-VGM) with an impedance-based electroanatomic mapping system EnSite (EnSite Velocity, St. Jude Medical, St. Paul, MN, USA) to identify critical channels in the CTI. Ablating this critical channel can lead to bidirectional block without completing an entire isthmus line.

2 Methods

Retrospective analysis of 25 patients (20 male, 5 female, mean age of 63) with typical AFL who underwent standard 3D mapping and ablation (group 1) was compared to 33 consecutive patients (29 male, 4 female, mean age 69) who underwent HD-VGM and ablation (group 2).

The study was approved by our local Institutional Review Board.

The diagnosis of typical AFL was based on the sawtoothed pattern of atrial activation on a 12-lead electrogram. The study was performed at two institutions with four primary operators (SN, WC, SS, RJ) and three St Jude representatives (NM, CB, AD). Patients were brought to the electrophysiology lab (EP lab) in the post-absorptive state in atrial flutter. Activation mapping and entrainment mapping of the RA were performed to confirm that the rhythm was CTI dependent AFL. For group 1 patients, the extent of 3D mapping to create geometry of the right atrium and CTI was performed at the operator's discretion. The only part of the procedure that was consistent was positioning the Livewire steerable decapolar catheter (St Jude Medical, Minnetonka, MN USA) in the coronary sinus (CS) as a reference catheter. Then, using the ablation catheter of the operator preference, the right atrium was mapped and CTI-dependent flutter was confirmed. The 3D map was used to identify the length of the isthmus, location of the TV and IVC, location of the ablation catheter, and location of the lesions. In group 2, A livewire steerable decapolar catheter was positioned in the CS as a reference catheter. For group 2 patients, all operators used the linear 2–2–2 mm

spaced 20-pole catheter (LiveWire, St Jude Medical, St. Paul, MN USA) to perform the HD-VGM of the RA with focus on the CTI. The IVC and the TV were identified and marked based on fluoroscopic and electrogram data. Ablation catheters for both groups were selected based on the operator's preference. In group 1 vs group 2, there were 12- vs 17 8-mm catheters, 13 vs 16 irrigated tip catheters, and 1 vs 3 contact sensing catheters. Ablation energy output, time, and temperatures varied with the particular catheter and their respective generators: Safire TX 8 mm, Safire BLU Duo, FlexAbility, and TactiCath 3.5-mm ablation catheter with the Ampere RF Ablation Generator (St Jude Medical, St Paul MN) and Blazer II XP 8-mm catheter with the Maestro 4000 Cardiac Ablation System (Boston Scientific, Natick MA).

2.1 High density mapping

Methods of acquiring and interpreting low voltage identification (LVID) signals with the EnSite mapping system can be found elsewhere [10–12]. In brief, the 3D map was set up using one of the CS electrograms as the electrical mapping reference based on the amplitude and consistency of the atrial electrograms. The roving activation interval window (RAI) was set up to detect 5 ms less than the tachycardia CL. The livewire was selected as the roving catheter and configured so the LAT and local electrogram voltages (EV) could be sampled from all defined bipolar signals simultaneously. The signal detection of absolute peak (Abs peak) was used on the roving catheter. Abs peak is defined as the largest amplitude, either positive or negative, of the bipolar signal and coincides with the $-dv/dt$ on a unipolar signal. Abs peak appropriately identifies the near-field deflection when multiple peaks are noted in a fractionated electrogram. The sensitivity was adjusted for the roving catheter to a maximum value of 10 mV to ensure that the largest amplitude bipolar signal was selected, rather than the first signal in our RAI. Intracardiac signals were assessed for noise, and a 60-Hz notch/noise filter was applied if 60-Hz noise was present. Interior and exterior projection values were set at 5 mm, rather than the default values of 15 mm. This keeps any intracavitary data from being used in the map. The interpolation value was also set between 5 mm, rather than the default value of 10 mm. Interpolation defines the radius of the color area surrounding each sampled point as well as how close two adjacent points must be to each other to have the computer define color between them. Duplicate points and points outside the interior projection window were automatically discarded. With this setting, regions of the 3D map containing missing LAT data was easily visible to the operator and targeted for further data collection.

After the data was collected, two methods of data interpretation were performed:

First the map was set to display eight isochronal color bands in the following activation pattern: white → red → orange → yellow → green → light blue → dark blue → purple corresponding to the eight activation times (Fig. 1). Each color band represents a temporal segment of the tachycardia cycle length as displayed in the isochronal time bar on the side of the screen. Areas with multiple color bands in a small distance represent areas of slower conduction whereas areas with rapid conduction will have larger bands of color.

Next in the map setting window, the cardiac triggered reference and LAT boxes are selected along with the LVID. The LVID slider is set to a default nominal value of 0.1 mV. Adjusting the LVID slider between 0.05 and 1.5 mV dynamically adjusts the peak to peak voltage represented on the LAT map. Areas with voltages under the LVID threshold appear gray, and voltages above the LVID threshold are represented by their respective color code on the LAT map. No timing values are displayed below the LVID threshold. By adjusting the LVID slider to a higher setting, only the voltages that exceed the threshold are apparent. In our method, the LVID was adjusted until a narrow bridge of conduction was noted in the CTI. If possible, ablation was performed in this area with the narrowest channel and between two gray areas, and therefore the shortest distance and the slowest conduction within the CTI (Fig. 1).

The distance from the TV to the IVC was measured along the line for ablation. The ablation lesions were also measured afterward to calculate the distance ablated. Ablation lesions terminated the AFL, and bidirectional block was achieved and confirmed without having to ablate the entire CTI. In addition, no “second lines” were needed to create bidirectional block.

2.1.1 2.2 Statistical analysis

All values are reported as mean ± standard deviation. Study and control groups were compared using parametric and non-parametric testing based as appropriate. Continuous variables were analyzed using Wilcoxon rank sum test. Fischer’s exact test was used to make comparisons between study and control groups. A p value ≤ 0.05 was considered significant. Statistical analysis was done using SAS Version 9.4 Software (SAS Institute Cary, NC).

3 Results

Fifty-eight patients were included in this study. In group 2 with at least 12 months (12–18 months) of follow-up, there were no recurrences. In group 1 with at least 12 months of follow-up, there were two recurrences of atrial flutter within the first 12 months. The procedure time was calculated from the time femoral access was achieved to the time the last ablation lesion creating bidirectional block was delivered.

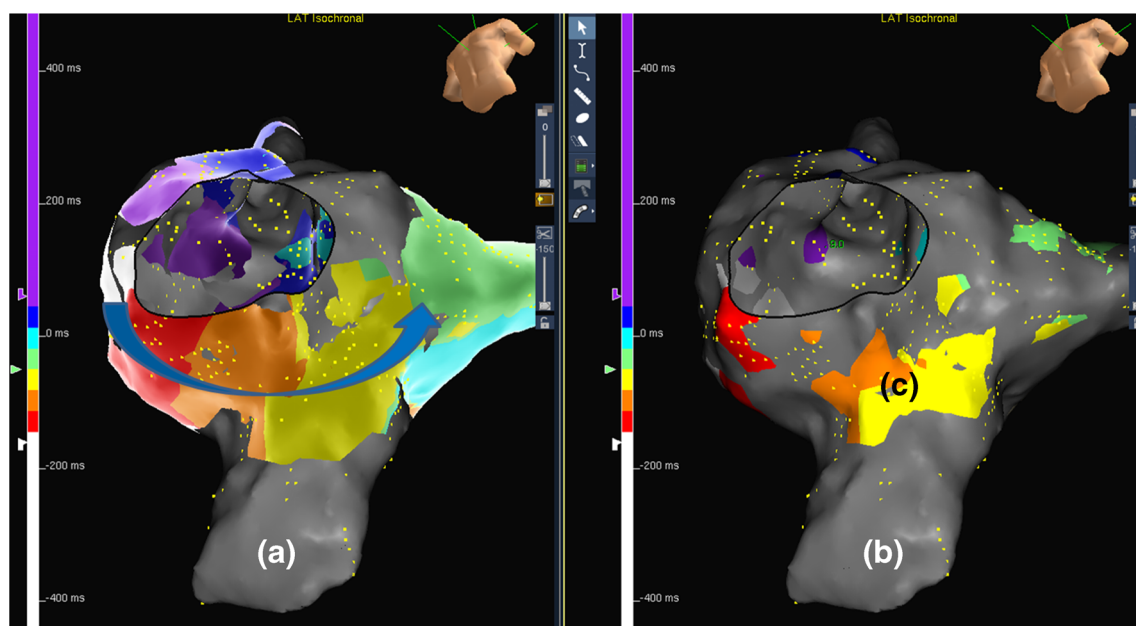


Fig. 1 HD-VGM map of AFL. CCL activation through the CTI indicated by the color progression (purple, white, red, orange, yellow, green, light blue, dark blue). Note: no slowing of conduction exists in this CTI. All color bands cover roughly equal distances which means conduction times are roughly the same. **a** A map with a LVID threshold

of 0.3 mV (gray color) typical setting for delineating low voltage in atrial tissue. **b** A map with a LVID threshold of 1.2 mV. All gray tissue falls below this threshold. **c** At the higher LVID setting threshold, a clear channel of higher voltage tissue can be seen through the isthmus. Targeting this area terminates the tachycardia

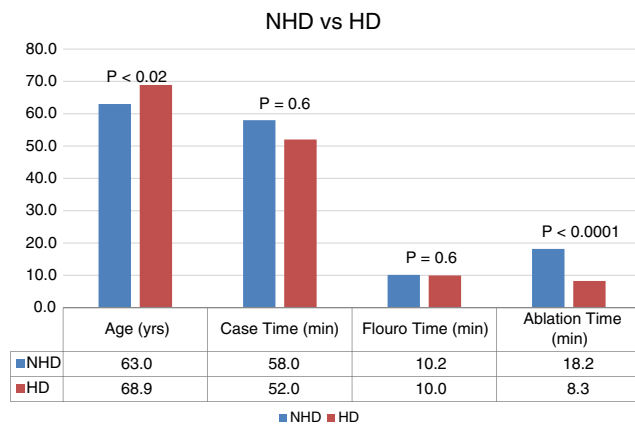


Fig. 2 Group 1 non-high density vs Group 2 high density

Comparisons between group 1 and group 2 are the following. The average age was 63 vs 69 years ($p < 0.02$), average total procedure times for the cases were 58 vs 52.0 ($p = 0.6$). Average fluoroscopy times were 10.2 vs 10.0 min ($p = 0.6$). An average of 22.7 lesions vs 5.5 lesions ($p < 0.0001$) was delivered. The average total ablation times were 18.2 vs 8.3 min ($p < 0.0001$) to achieve bidirectional block (Fig. 2). For group 2, an average of 5197 points were collected and 1421 points used in 12.0 min to create an HD map of the CTI. The average length of CTI was 47.0 vs 46.1 mm ($p = 0.87$). The length of the ablation lesions was 46.1 vs 32.6 mm ($p < 0.0003$). In group 1, the total length of the isthmus was ablated, whereas in group 2, only 71% of the isthmus was ablated. Average mapping to termination time in group 2 was 23.0 min (7–70 min) from the beginning of mapping to termination of flutter with bidirectional block. Detailed statistics are listed in Table 1.

In group 2, there were 25 cases with predominantly rapid uniform conduction through the CTI and the tachycardia terminated in 60% of cases (15/25) without slowing of the cycle length (CL). In other words, there was no change in the CL of the tachycardia until termination of the AFL to sinus rhythm. The other eight patients had

slowing of the tachycardia CL (defined as a CL change greater than 10 msec) during the ablation lesions before termination in six of eight patients. In these patients, the CL increased as we ablated the isthmus. The overall activation sequence of the tachycardia did not change despite CL prolongation which indicated that conduction continued through the CTI but had shifted to the slower conducting fibers within the CTI before termination. The increase in CL usually occurred from the middle of the CTI towards the IVC boundary. Although there was termination, bidirectional block did not usually occur until the line was completed. This may suggest that although tachycardia was occurring through these preferential fibers, other fibers are still capable of conduction. Functional lines of block were also noted in the critical isthmus in some of these subjects (Fig. 3).

4 Discussion

Our study shows that HD-VGM method can improve on the ablation strategy for AFL. By incorporating voltage and timing data, a more precise location for the ablation lesions can be determined. By doing so, we improve on the distance ablated and time of ablation.

Previous studies have shown that typical AFL is a re-entrant circuit involving the RA [4, 13, 14]. Multiple studies followed showing that there was a critical area of slow conduction in the CTI which maintained the tachycardia. [4, 13, 15, 16] Since Feld et al. showed that ablation in the critical area inferior or posterior to the CS ostium could successfully terminate AFL, the procedure has been performed in this manner [6]. Ablation using fluoroscopy has been performed empirically at 6 o'clock on the TV in LAO 30° view from the TV to the IVC to reduce the risk of damage to the compact AV node [17]. This empiric method has been a successful ablation

Table 1 Patient characteristics

Data	Group 1 (non-HD)	Group 2 (HD)	<i>p</i> Value
Number	25	33	
M/F (<i>n</i>)	20/5	29/4	0.4
Age (years)	63 ± 9.5	69 ± 9.2	<0.02
CHADSVASC Score	1.2	1.9	<0.02
Procedure time (min)	58 ± 27 (27–132)	52 ± 18 (29–105)	0.6
Ablation time (min)	18.2 ± 9.2 (1.5–45.3)	8.3 ± 4.0 (2.5–18)	<0.0001
Number of lesions (<i>n</i>)	23 ± 16.9 (3–60)	5.5 ± 4.2 (1–18)	<0.0001
Fluoroscopy time (min)	10.2 ± 8.4 (2–36.2)	10.0 ± 5.9 (2–19.2)	<0.6
Isthmus length (mm)	47.0 ± 13 (33–72)	46.1 ± 10 (29–66)	0.87
Isthmus ablated (mm)	47.0 ± 13 (32–74)	32.6 ± 10 (17–53)	<0.0003
Mapping time (min)	N/A	12.0 (6–20)	

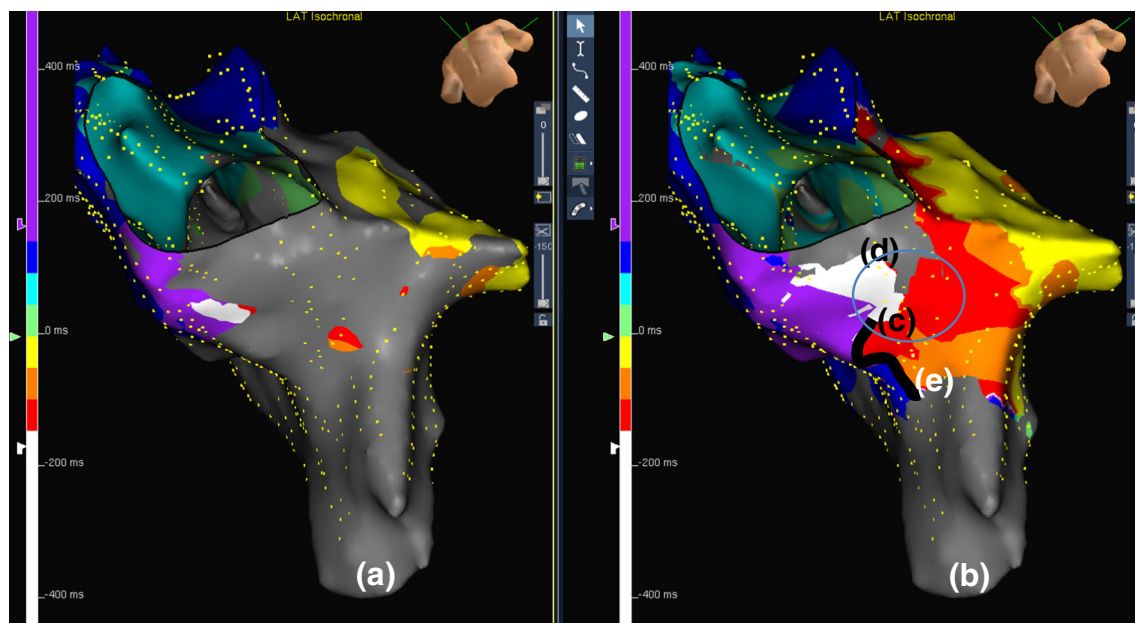


Fig. 3 Patient with two different voltage settings used to define the isthmus. Map (a) represents a LVID setting of 0.3 mV. At this setting, it is difficult to see conduction patterns due to the electrograms falling under the voltage threshold. Map (b) represents a LVID setting of 0.05 mV. By adjusting the sensitivity, propagation through the isthmus channel (c) can be identified. Following the color pattern, the channel can be seen where

purple leads to white then to red between the low voltage area (d) at the tricuspid annulus, and e an area of functional block (dark line). As these two colors are not in sequence (dark blue next to orange), it is indicative of an area of block. Ablation of the channel (c) blue circle terminates the tachycardia

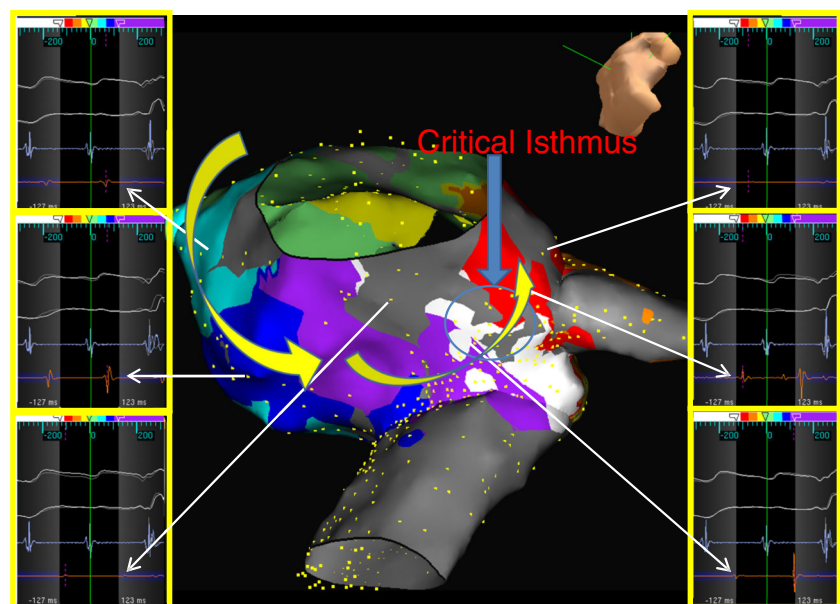
approach; however, recent studies have shown that targeted ablation of the fiber bundles based on maximum electrogram voltage criteria is also an effective method and can reduce ablation times [18–23].

Bailin et al. used a voltage gradient method to identify areas of heterogeneous voltage within the CTI to ablate. Both our strategy and Bailin's show that specific bundle fibers can be ablated to produce bidirectional block

without ablating the entire isthmus. They were able to quickly create an electroanatomic map of the CTI without significantly increasing procedure time [18, 19]. By doing so, they were able to decrease the ablation time.

Similar to Winkle's recent publication, we have also reported on high density mapping method in our lab to identify the slow zone in atypical flutter circuits [11, 12]. This HD-VGM method of mapping and interpretation is

Fig. 4 Electrogram breakdown for the areas from lateral to medial along the isthmus, yellow arrow. Note the channel which appears on the medial side based on lower voltage surrounding tissue. Low-V ID set at 0.3 mV. Adjusting the LVID determines the path of least resistance, an ablation target can be identified in the critical isthmus of this AFL



different than the currently accepted methods because it utilizes a voltage map overlaid on a local activation timing map. By combining both maps, the highest voltage within the critical slow zones of conduction can be rapidly identified and targeted for ablation. It is this combination of the voltage map overlaid on the activation map that has not previously been evaluated in AFL. We are able to visualize on a 3D map the maximum voltage areas noted in the prior studies and target these areas first. By doing so, we can see changes in CL, and at times termination of the tachycardia [18–23].

The average additional mapping time in our study was 12.0 min. By adjusting the LVID to show only the highest voltage in the area, we may be targeting the largest muscle bundle capable of conduction (Fig. 4). Ablating only the fibers responsible for propagation reduces the area ablated and decreases overall ablation time. [18–22, 24] This was negated by the fact that our ablation times were much shorter by identifying the shortest area for ablation. We only had to ablate an average of only 71% of the isthmus compared to the traditional approach (TV-IVC) to achieve bidirectional block.

The HD group was older than the non-HD group 63 vs 69 years ($p < 0.02$), and the CHADSVASC score was higher 1.9 vs 1.2 ($p < 0.02$). Even though the age and CHADSVASC score was higher for the HD group, the isthmus length was not statistically significant between the two groups. The HD cohort was older and sicker, and therefore, HD method may have

been even more statistically significant if the groups were of comparable age and CHADSVASC score.

4.1 Group 2

Studies have also shown that the length of the isthmus is greater in patients with AFL. The mean length of the isthmus in group 2 was 46.1 mm consistent with prior studies [25]. This stretching of the isthmus may play a role in allowing for anisotropic conduction [25, 26]. The electro-anatomic data is consistent with prior anatomic studies noted by Waki and Cabrera [27, 28]. The CTI can be divided into three sections. Anterior near the TV is mostly smooth muscular tissue. The middle floor of the CTI has muscular fibers separated by fibrous tissue, while the posterior segment near the Eustachian ridge (ER) and IVC is composed mostly of fibrous and fatty tissue with minimal muscular fibers [5, 28, 29]. Redfearn et al. found that in 67% of patients, there was a discrete jump in conduction with RF application of these muscle bundles. Consistent with Redfearn et al., in our series, 64% (21/33) of cases had a change in CL before termination. This usually occurred in the posterior 2/3 of the CTI [18].

In 78% (26/33) of the cases, there was evidence of low voltage (gray areas) within the CTI. In 23 of the 33 cases, there were low voltage areas at the anterior portion of the isthmus near the TV annulus (Fig. 5). Instead of using the standard approach of beginning the ablation where the TV annulus was anatomically identified using fluoroscopy and electrograms, the ablation line was started more distally in the isthmus where healthy voltages were present based on LVID. This helped shorten the length of the ablation line and number of lesions. After termination of the tachycardia, gaps in the ablation line were not noted in this anterior gray area when confirming bidirectional block. This suggests that the gray areas are fixed areas of block versus functional areas of block. If it were due to functional block, propagation gaps through this area would have occurred when we paced after we terminated the tachycardia. If the TV annulus was underestimated when creating the geometry and healthy tissue capable of propagation was not ablated, bidirectional block would not be present in this area. It is possible that this low voltage area is only present in patients with atrial myopathy predisposing them to AFL.

5 Conclusion

A rapidly collected HD-VGM of the CTI decreases the ablation time, and length of the ablation line without changes in overall success rate. Bidirectional block can be achieved without ablating the entire CTI line. This

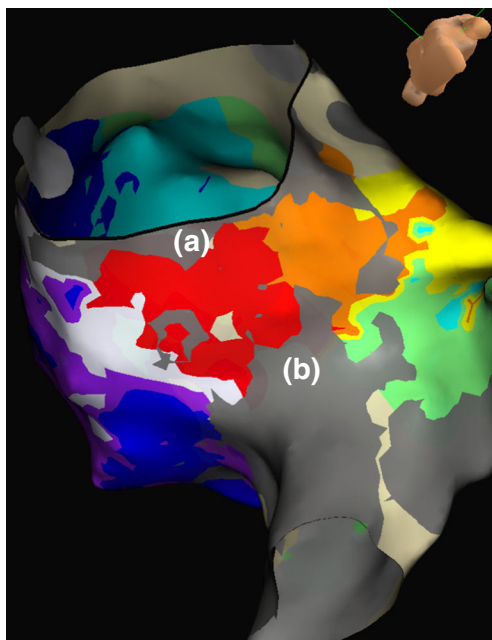


Fig. 5 Most patients had lower voltage areas in two distinct regions. **a** The low voltage area seen at the anterior portion of the isthmus representing scar near the TV annulus. **b** The posterior segment near the ER and IVC

study demonstrates that high density mapping of the CTI may improve on ablation techniques and further studies should be performed.

6 Limitations

This was not a randomized study and operator bias including experience may have been introduced. This was not an age matched cohort and the age difference was statistically significant. The HD group was older and with a higher CHADSVASC score compared to the control group. The data points were not individually analyzed manually by the operator. This was done to increase the speed of data collection and analysis. The tradeoff for the increased speed is that errors in notation could have been made and accounted for in the 3D maps.

Acknowledgements We thank Kimberly Oaks for helping edit the paper.

Compliance with ethical standards

Conflict of interest Drs. Sundaram and Choe are on the speaker's bureau and consultants for St. Jude Medical. In addition, Drs. Sundaram and Choe have received a research grant from St. Jude Medical, Asia Division to study the genetic basis of Brugada Syndrome in Cambodia. This conflict is not relevant to the article.

Dr. Jordan is a consultant for St Jude Medical.

N. Mullins, C. Boorman, and A Davies receive salary support from St. Jude Medical.

Dr. Sunil Nath and Alex C Tiftickjian have no conflict of interest to declare.

This research did not receive any specific grant from funding agencies in the public, commercial, or not-for-profit sectors.

Ethical approval All procedures performed in the study involving human participants were in accordance with the ethical standards of the institutional research committee and with the 1964 Helsinki declaration and its later amendments or comparable ethical standards.

For this type of study, formal consent is not required.

References

- Jolly WA, Ritchie WT: Auricular Flutter and Fibrillation Heart. 1910–1911 2 177.
- Lewis T. Observations on a curious and Not Uncommon Form of Extreme Acceleration of the Auricle. "Auricular Flutter.". Heart. 1912–1913;4:–171.
- Blackford JM, Willius F. Auricular Flutter. Arch Int Med. 1918;21: p147–65.
- Olshansky B, Okumura K, Hess P, Waldo A. Demonstration of an area of slow conduction in human atrial flutter. J Am Coll Cardiol. 1990;16:1639–48.
- Gami AS, Edwards WD, Lachman N, Friedman PA TD, Munger TM, Hammill SC, et al. Electrophysiological anatomy of typical atrial flutter: the posterior boundary and causes for difficulty with ablation. J Cardiovasc Electrophysiol. 2010;21:144–9.
- Feld G, Fleck P, Chen PS, Boyce K, Bahnson T, Stein J, et al. Radiofrequency catheter ablation for the treatment of human type I atrial flutter. Identification of a critical zone in the reentrant circuit by endocardial mapping techniques. Circulation. 1992;86:1233–40.
- Cosio FG, Lopez-Gil M, Coicolea A, Arribas F, Barroso JL. Radiofrequency ablation of the inferior vena cava-tricuspid valve isthmus in common atrial flutter. Am J Cardiol. 1993;71:705–9.
- Poty H, Saoudi N, Nair M, Anselme F, Letac B. Radiofrequency catheter ablation of atrial flutter. Further insights into the various types of isthmus block: application to ablation during sinus rhythm. Circulation. 1996;94:3204–13.
- Anselme F, Savouire A, Cribier A, Saoudi N. Catheter ablation of typical atrial flutter. A randomized comparison of 2 methods for determining complete bidirectional isthmus block. Circulation. 2001;103:1434–9.
- Ensite Velocity System Instructions for Use 2011 v.3.0.1 : p161.
- Winkle RA, Moskovitz R, Mead RH, Engel G, Kong MH, Fleming W, et al. Ablation of atypical atrial flutter using ultra high density-activation sequence mapping. J Interv Card Electrophysiol. 2017;48:177–84.
- Sundaram S, Choe W, Mullins N, Boorman C, Nath S. Catheter ablation of atypical atrial flutter: a novel 3D anatomic approach to quickly localize and terminate atypical atrial flutter. Poster Presentation HRS May 2016. PO 003–110. Heart Rhythm, Vol.13, No.5 May Supplement 2016: S295.
- Cosio F, Lopez-Gil M, Goicolea A, Arribas F. Electrophysiologic Studies in Atrial Flutter. Clin Cardiol. 15:667–73.
- Olgin J, Kalman J, Fitzpatrick A, Lesh M. Role of right atrial endocardial structures as barriers to conduction during human type I atrial flutter. Activation and entrainment mapping guided by Intracardiac echocardiography. Circulation. 1995;92:1839–48.
- Klein GJ, Guiraudon GM, Sharma AD, Milstein S. Demonstration of macroreentry and feasibility of operative therapy in the common type of atrial flutter. Am J Cardiol. 1986;57:587–91.
- Saoudi N, Atallah G, Kirkorian G, Touboul P. Catheter ablation of the atrial myocardium in human type I atrial flutter. Circulation. 1990;81:762–71.
- Asirvatham SJ. Correlative anatomy and electrophysiology for the interventional electrophysiologist: right atrial flutter. J Cardiovasc Electrophysiol. 2009;20:113–22.
- Redfearn DP, Skanes AC, Gula LJ, Krahn AD, Yee R, Klein GJ. Cavotricuspid isthmus conduction is dependent on underlying anatomic bundle architecture: observations using a maximum voltage-guided ablation technique. J Cardiovasc Electrophysiol. 2006;17: 823–38.
- Bailin SJ, Johnson WB, Jumrussirkul P, Sorentino D, West R. A new methodology for atrial flutter ablation by direct visualization of cavotricuspid conduction with voltage gradient mapping: a comparison to standard technique. Europace. 2013;15:1013–8.
- Maruyama M, Kobayashi Y, Miyauchi Y, Iwasaki Y, Morita N, Miyamoto S, et al. Mapping-guided ablation of the cavotricuspid isthmus: a novel simplified approach to radiofrequency catheter ablation of isthmus-dependent atrial flutter. Heart Rhythm. 2006;3:665–73.
- Subbiah RN, Gula LJ, Krahn AD, Posa E, Yee R, Klein GJ, et al. Rapid ablation for atrial flutter by targeting maximum voltage-factors associated with short ablation times. J Cardiovasc Electrophysiol. 2007;18:612–6.
- Gula LJ, Redfearn DP, Veenjuyzen GD, Krahn AD, Yee R, Klein GJ, et al. Reduction in atrial flutter ablation time by targeting maximum voltage: results of a prospective randomized clinical trial. J Cardiovasc Electrophysiol. 2009;20:1108–12.
- Lewalter T, Lickfett L, Weiss C, Mewis C, Spencker S, Jung W, et al. "largest amplitude ablation" is the optimal approach for typical

- atrial flutter ablation: a subanalysis from the AURUM 8 study. *J Cardiovasc Electrophysiol*. 2012;23:479–85.
24. Mechulan A, Gula LJ, Klein GJ, Leong-Sit P, Obeyesekere M, Krahn AD, et al. Further evidence for the “muscle bundle” hypothesis of Cavotricuspid isthmus conduction: physiological proof, with clinical implications for ablation. *J Cardiovasc Electrophysiol*. 2013;24:47–52.
 25. Cabrera JA, Sanchez-Quintana D, Ho SY, Medina A, Wanguemert F, Gross E, et al. Angiographic anatomy of the inferior right atrial isthmus in patients with and without history of common atrial flutter. *Circulation*. 1999;99:3017–23.
 26. Boineau JP, Schuessler RB, Mooney CR, Miller CB, Wylds AC, Hudson RD, et al. Natural and evoked atrial flutter due to circus movement in dogs: role of abnormal pathways, slow conduction, nonuniform refractory period distribution and premature beats. *Am J Cardiol*. 1980;45:1167–81.
 27. Waki K, Saito Tsukasa S, Becker AE. Right atrial flutter isthmus revisited: normal anatomy favors nonuniform anisotropic conduction. *J Cardiovasc Electrophysiol*. 2000;11:90–4.
 28. Cabrera JA, Sanchez-Quintana D, Ho SY, Medina A, Anderson RH. The architecture of the atrial musculature between the orifice of the inferior Caval vein and the tricuspid valve: the anatomy of the isthmus. *J Cardiovasc Electrophysiol*. 1998;9:1186–95.
 29. Scaglione M, Caponi D, Di Donna P, Riccardi R, Bocchiardo M, Azzaro G, et al. Typical atrial flutter ablation outcome: correlation with isthmus anatomy using intracardiac echo 3D reconstruction. *Europace*. 2004;6:407–17.